Tetrahedral Stars as Flexible Basis Clusters in sp-Bonded Intermetallic Frameworks and the Compound $BaLi_7Al_6$ with the $NaZn_{13}$ Structure

Ulrich Häussermann,* Christer Svensson, and Sven Lidin

Contribution from the Department of Inorganic Chemistry 2, Lund University, P.O. Box 124, S-22100 Lund, Sweden

Received September 23, 1997. Revised Manuscript Received December 29, 1997

Abstract: The cluster units obtained by the capping of all faces of a tetrahedron (tetrahedral star, TS) and a trigonal bipyramid (double tetrahedral star, DTS) are used as building units to describe and rationalize framework structures found in the intermetallic structure types NaBa, $NaZn_{13}$, Th_6Mn_{23}, $Ba_2Li_{4.21}Al_{4.79}$, $BaHg_{11}$, $BaCd_{11}$, $Cr_{23}C_6$, β-Mn, $Ba_3Li_3Ga_{4.1}$, $BaLi_4$, $CaZn_3$, $EuMg_{5.2}$, $ErZn_5$, Sr_3Mg_{13}, and $Sr_9Li_{17.5}Al_{25.5}$. The electronic requirements for optimum structural stability of these frameworks in the case of sp-bonding have been investigated with the simple tight-binding Hückel model. As a result the networks exhibit a pronounced maximum of stability in the range of 2.1−2.6 electrons per atom with the particular optimum values slightly depending on the kind of basis cluster and its connectivity. Considering the sp-bonded representatives of the above mentioned structure types, the frameworks described by the basis clusters TS and DTS are usually formed by the divalent metals Be, Mg, Zn, Cd, and Hg or a combination of a mono- and a trivalent metal, e.g., (Li,Al), (Cu,Al), or (Ag,Al). More electropositive atoms, like the heavier alkaline earth metals Ca, Sr, and Ba, are embedded in such frameworks. When applying a formal electron transfer from these atoms to the slightly more electronegative framework forming atoms, the obtained values for the framework valence electron concentration are very close to the calculated optimum ones. Therefore it is argued that this family of intermetallic compounds can still be interpreted as electron compounds following the Zintl−Klemm concept. The new representative $BaLi_7Al_6$, which has been synthesized by fusion of the elements and characterized by single-crystal X-ray diffraction methods, supports this idea. $BaLi_7Al_6$ is isotypic to $NaZn_{13}$ ($Fm\bar{3}c$, $a = 12.9377(9)$ Å, $Z = 8$) with the Zn sites mixed occupied by Li and Al atoms.

1. Introduction

In the past few years research on polar intermetallic compounds has developed into one of the most exciting fields in inorganic chemistry. A wealth of novel and peculiar structures has been discovered and unforeseen bonding patterns based on multicenter bonding has been analysed.[1−4] This has led to an increased understanding of chemical bonding in systems at the metal nonmetal border reflecting the transition from covalent to metallic bonding.[5,6]

Polar intermetallics are compounds formed between two or more metallic elements with distinctly different electronegativities. In particular the electronegative component is one of the group 13 elements which are called triels (**Tr**), and the more electropositive counterpart is represented by an alkali metal (**A**) or/and an alkaline earth metal (**Ae**) or a trivalent rare-earth element (**R**). In these systems triel atoms are reduced by the electropositive component and thus obtain a valence electron concentration (VEC, number of valence electrons of a formula unit per Tr atom) which enables them to fit the electronic requirement for the formation of a remarkable variety of sp-bonded networks, clusters, or cluster frameworks. The formal electron transfer is in the spirit of the Zintl−Klemm concept, and indeed many of the polar intermetallics can be counted as Zintl phases, especially when applying the criterion diamagnetism for defining (closed-shell) Zintl phases.[3] However, a rather large number of polar intermetallics exhibit small deviations from the electron count which would follow from the Zintl−Klemm concept. This indicates that other contributions to structural stability, like packing and interrelated size effects, gain importance compared to the stability-determining VEC in Zintl phases. But still the Zintl−Klemm concept provides an excellent starting point for the interpretation and prediction of bonding motifs in these compounds.

One may roughly distinguish between three different kinds of Tr substructures occurring in the polar intermetallics: open networks found in the systems Ae/Tr in a range of VEC between 3.5 and 5.0; isolated clusters in the systems A/Tr and A/A′/Tr for values of VEC between 3.6 to 5.0; and in the same systems frameworks of clusters in a range of VEC between 3.14 and 3.6. Characteristically these clusters represent deltahedral units or are related to them and thus correspond to entities with a

(1) Belin, C.; Tillard-Charbonell, M. *Prog. Solid State Chem.* **1993**, *22*, 59 and references therein.

(2) Eisenmann, B.; Cordier, G. In *Chemistry, Structure and Bonding of Zintl Phases and Ions*; Kauzlarich, S. M., Ed.; VCH Publishers: New York, 1996; Chapter 2 and references therein.

(3) Corbett, J. D. In *Chemistry, Structure and Bonding of Zintl Phases and Ions*; Kauzlarich, S. M., Ed.; VCH Publishers: New York, 1996; Chapter 3 and references therein.

(4) Nesper, R. *Habilitationsschrift*; University of Stuttgart: Stuttgart, Germany, 1988; (in German).

(5) Nesper, R. *Angew. Chem., Int. Ed. Engl.* **1991**, *30*, 789 and references therein.

(6) Miller, G. J. In *Chemistry, Structure and Bonding of Zintl Phases and Ions*; Kauzlarich, S. M., Ed.; VCH Publishers: New York, 1996; Chapter 1 and references therein.

S0002-7863(97)03335-0 CCC: $15.00
Published on Web 04/14/1998

certain electron requirement. In cluster frameworks the clusters are basically linked via exo-bonds. From theoretical considerations it is expected that a VEC around 3.0 represents a limiting value for the formation of deltahederal cluster units.[7] A further decrease of VEC is, in principle, possible by the replacement of Tr atoms by group 12 (zinc group, E12) or even group 11 (copper group, E11) elements when assuming that the transition metal d electrons do not participate in the bonding (e.g., $K_{34}[Zn_{20}In_{85}]$,[8] $Na_{36}[Ag_7Ga_{73}]$,[9] $Na_{34}[Cu_7Cd_6Ga_{92}]$[10]). However, in the obtained compounds the VEC decreased hardly below 3.0, and most of the (complex) substructures are still based on exo-bonded deltahedral clusters (preferably icosahedral units), although new moieties in the form of peculiarly fused or fragmented icosahedra occur. The question arises if the A/E11(E12)/Tr systems designate a borderline for intermetallic compounds with substructures mainly governed by VEC or if there are even electron poorer systems following the Zintl−Klemm concept. Clearly, a further decrease of VEC should result in other structural motifs than deltahedral cluster units or derivatives of them. What kind of building principles do electron poorer systems with VEC < 3 follow and—most importantly—what is the composition of such systems?

Recently we described the Mg frameworks in compounds between the heavier alkaline earth metals (Sr, Ba) and magnesium, like Sr_3Mg_{13}, $SrMg_{5.2}$, and Ba_6Mg_{23}, in terms of two simple basis clusters and found a pronounced maximum of stability for values of VEC around 2.5 electrons per framework atom.[11] This electron count coincides with the Zintl−Klemm concept and adjoins indeed that of the polar intermetallics with substructures based on deltahedral clusters. The basis clusters we used to describe the Mg frameworks are the all-face capped tetrahedron (tetrahedral star, TS) and the all-face capped trigonal bipyramid (double tetrahedral star, DTS). In this article we investigate more systematically the relation between geometrical structure, electron count, and structural stability of sp-bonded intermetallics with frameworks based on these TS and DTS clusters. We add, with the new compound $BaLi_7Al_6$, a further example and interpret this class of compounds as the electron poorest systems following the Zintl−Klemm concept.

2. Experimental and Calculational Details

2.1. Synthesis. The compound $BaLi_7Al_6$ was prepared by melting mixtures of the pure elements with the compositions $BaLi_5Al_8$, $BaLi_7Al_6$, $BaLi_8Al_5$ (Li (99.9%, Aldrich), Al (99.9%, Aldrich), Ba (99.9%, Alfa)) in stainless steel ampoules which had been weld-sealed under Ar atmosphere. The mixtures were heated to 800 °C for 8 h, followed by slow cooling (15 °C/h) to room temperature. The products of the reactions, being brittle and of silver grey color, were examined inside a glovebox filled with purifed Ar. The characterization by X-ray powder diagrams revealed an almost homogenous product with traces of the compound $Ba_2Li_{4.21}Al_{4.79}$.[11] The phase width of the new compound $BaLi_7Al_6$ is assumed to be very narrow, which we concluded from the fact that in powder patterns of samples with different composition the positions of the lines belonging to $BaLi_7Al_6$ were not changed. Further, the refined Li/Al ratios of two crystals from the samples $BaLi_7Al_6$ and $BaLi_8Al_5$ were found to be virtually identical (cf. section 3). Crystals of $BaLi_7Al_6$ are remarkably stable in dry air.

Table 1. Crystallographic Data for $BaLi_7Al_6$

empirical formula	$BaLi_7Al_6$
space group	$Fm\bar{3}c$ (no. 226)
lattice constant, Å	$a = 12.9377(9)$
vol, Å^3	2165.6(1)
Z	8
calc density, g/cm^3	2.126
T, K	295
wavelength, Å^{-1}	0.71069 (Mo Kα)
absorptions coeff, mm^{-1}	4.07
$R1^a$ [$\lvert F\rvert^2 \geq 2\sigma(\lvert F\rvert^2)$]	0.031
wR^b [$\lvert F\rvert^2 \geq 2\sigma(\lvert F\rvert^2)$]	0.075

[a] $R1 = [\sum(|F_o| - |F_c|)]/\sum|F_o|$. [b] $wR = \{[\sum w(F_o^2 - F_c^2)^2]/\sum w(F_o^2)^2\}^{1/2}$. $w = [\sigma^2(|F_o|^2 + (aP)^2 + bP]^{-1}$. $P = (F_o^2(\geq 0) + 2F_c^2)/3$ ($a = 0.0451$, $b = 3.04$).

Table 2. Positional Coordinates and Isotropic Displacement Parameters for $BaLi_7Al_6$

atom	site	x	y	z	SOF	U_{iso}, 10^4 Å^2
Ba	8a	1/4	1/4	1/4	1	302(2)
M1	8b	0	0	0	Al 0.26(3) Li 0.74(4)	342(31)
M2	96i	0	0.1775(1)	0.1145(1)	Al 0.473(7) Li 0.527(7)	312(5)

Table 3. Anisotropic Thermal Displacement Parameters (10^4 Å^2) for $BaLi_7Al_6$

atom	U_{11}	U_{22}	U_{33}	U_{12}	U_{13}	U_{23}
Ba	302(2)	302(2)	302(2)	0	0	0
M1	342(31)	342(31)	342(31)	0	0	0
M2	343(9)	294(9)	300(9)	39(7)	0	0

2.2. Single Crystal Structure Determination. A suitable single crystal for structure determination (dimension 0.09 × 0.15 × 0.05 mm) was picked up from the sample with the composition $BaLi_7Al_6$ and sealed in a Lindemann glass capillary. The data were collected on a Huber diffractometer with the ω-2θ scan type at room temperature with graphite-monochromated Mo K_α radiation. Cell constants were obtained from a least-squares refinement of the setting angle of 38 centred reflections. The data set included one hemisphere in the range of $2° \leq 2\theta \leq 70°$ (index limits $-20 \leq h \leq 20$; $-20 \leq k \leq 20$; $0 \leq l \leq 20$). Some details of the single crystal data collection and refinement are listed in Table 1. The space group $Fm\bar{3}c$ was assigned on the basis of the systematic absences and the statistical analysis of the intensity distributions. An analytical absorption correction was performed which improved $R_{int}(F_o^2)$ from 0.095 to 0.065 (232 unique reflections; 4953 total reflections). The structure of $BaLi_7Al_6$ was refined successfully as a variation of the $NaZn_{13}$ structure type assuming a mixed occupation of Li and Al atoms on the Zn sites (least-squares refinement on F^2 (program SHELXL-93[12])). The composition of the compound was determined from the refined Li/Al ratios. The residual electron densities in the last difference Fourier map ranged between +1.5 e/Å^3 and −0.37 e/Å^3. In Table 2 the atomic positions and isotropic displacement factors are given. Table 3 lists the anisotropic displacement factors and Table 4 the relevant atomic distances.

2.3. Electronic Structure Calculation. Electronic structure calculations were performed within the framework of simple tight-binding (TB) Hückel theory by solving the secular determinant $|H_{ij}(\vec{k}) - \epsilon I| = 0$ with the unit matrix I and the

(7) Burdett, J. K.; Canadell, E. *J. Am. Chem. Soc.* **1990**, *112*, 7207.
(8) Cordier G.; Müller V. *Z. Naturforsch.* **1995**, *50b*, 23.
(9) Tillard-Charbonell, M.; Chahine, A; Belin, C. *Z. Kristallogr.* **1993**, *208*, 372.
(10) Chahine, A; Tillard-Charbonell, M.; Belin, C. *Z. Kristallogr.* **1994**, *209*, 542. *90*, 270; **1993**, *206*, 310.
(11) Häussermann, U.; Wörle, M.; Nesper, R. *J. Am. Chem. Soc.* **1996**, *118*, 11789.
(12) Sheldrick, G. M. *SHELXL-93 Program for the Refinement of Crystal Structures*; University of Göttingen: Göttingen, Germany, 1993.

atomic parameters of Al ($H_{4s4s} = -12.3$ eV, $H_{4p4p} = -6.5$ eV, $\zeta_{3s} = \zeta_{3p} = 1.167$). The resonance integrals were approximated by the Wolfsberg-Helmholtz formula $H_{ij} = {}^1/_2 KS_{ij}(H_{ii} + H_{jj})$ with $K = 1.75$, and appropriate meshes between 10 and 80 *k*-points of the irreducible wedges (depending on the unit cell content) were used.[13] In order to compare structural energy differences within the TB formalism we applied the energy difference theorem of Pettifor[14] and scaled the electronic density of states of the framework structures by an isotropic change of the bond lengths until their second moments adopted the same value (second moment scaling[15]). The second moment, which represents a quantity proportional to the repulsive energy in these systems, was chosen as the mean value of fcc-Al and the Al framework in $BaAl_4$ at their experimental equilibrium volumes. The value obtained was supposed to present a mean value for the frameworks under consideration. For investigating the influence of VEC on structural stability we used the simple cubic (sc) structure as a neutral reference system[16] and calculated energy difference curves relative to this structure. The peculiarity of the sc structure is that its sp-density of states exihibits only little structuring (no gaps or pseudogaps indicating strong bonds nor a long tail toward low energies indicating a prevalence of three-membered rings). This ensures an almost equal influence on the various difference curves and thus unbiased values of the maxima/minima and is comparable to the use of a skew-rectangular density of states as a neutral reference system.[17]

3. The Compound $BaLi_7Al_6$

$BaLi_7Al_6$ crystallizes with the $NaZn_{13}$ structure. This structure can be described as a CsCl type arrangement of centered icosahedra of zinc atoms and Na atoms (Figure 1a). Na is coordinated by 24 Zn atoms all with the same distance from the central atom, and the polyhedron is called a "snub cube" (Figure 1b).[18]

In $BaLi_7Al_6$ the icosahedra-forming position is approximately equally occupied by Li and Al atoms (Li: 53(1)%; Al: 47(1)%), but the centering position exhibits a clear tendency to be occupied by the monovalent Li (Li: 74(4)%; Al: 26(3)%) (Table 2). The composition of the crystal adds up to $BaLi_{7.1(1)}Al_{5.9(1)}$. The investigated crystal presented in Table 2 was selected from a sample with the nominal composition $BaLi_7Al_6$. For a crystal from a sample with the composition $BaLi_5Al_8$ we refined the following Li/Al ratios: 0.52(1)/0.48(1) for the icosahedra-forming position and 0.71(5)/0.29(4) for the centering position. This yields a crystal composition of $BaLi_{7.0(2)}Al_{6.0(2)}$, indicating only a narrow phase with for the compound $BaLi_7Al_6$.

Around 100 compounds are reported to crystallize with the $NaZn_{13}$ type,[19] which preferentially forms with the divalent metals of highest electronegativity Be, Zn, or Cd as the majority component and a large A, Ae, or lanthanoid counterpart. In ternary compounds the divalent majority component is replaced by combinations of Cu/Al, Cu/Ga, Cu/In, or Ag/Al. The combination Li/Al has not been observed until in the compound $BaLi_7Al_6$. Remarkably, of the sp-bonded ternary compounds only $LaCu_xAl_{13-x}$ is reported with a considerable phase width ($5.5 \leq x \leq 10.0$).[20] The other compounds with mono-(I) and trivalent(III) metals on the sites of the majority component have—with the exception of the compound $BaCu_5Al_8$[21]—I/III ratios of either 1:1 or 7:6.[19] Further, the icosahedra-centering position in a number of compounds was found to be occupied exclusively by the monovalent metal. Both trends of the sp-bonded ternaries—a narrow phase width and the preferency of the icosahedra-centring position for the monovalent metal—are also reflected by the new compound $BaLi_7Al_6$.

In the series of Ba compounds with the $NaZn_{13}$ type ($BaBe_{13}$, $BaCu_{13}$, $BaCu_5Al_8$, $BaZn_{13}$, $BaLi_7Al_6$), cell parameters range from 10.485 Å ($BaBe_{13}$) to 12.938 Å ($BaLi_7Al_6$). It has been pointed out by Nyman and Andersson that the size of unit cell and the snub cube around the large atoms are solely determined by the bonding distances in the icosahedra.[22] Thus, in this series Ba exhibits a remarkable flexibility in the size of its coordination polyhedron as elucidated by the distances $d_{Ba-Be} = 3.11$ Å in $BaBe_{13}$ and $d_{Ba-M} = 3.80$ Å in $BaLi_7Al_6$ (Table 4). Because

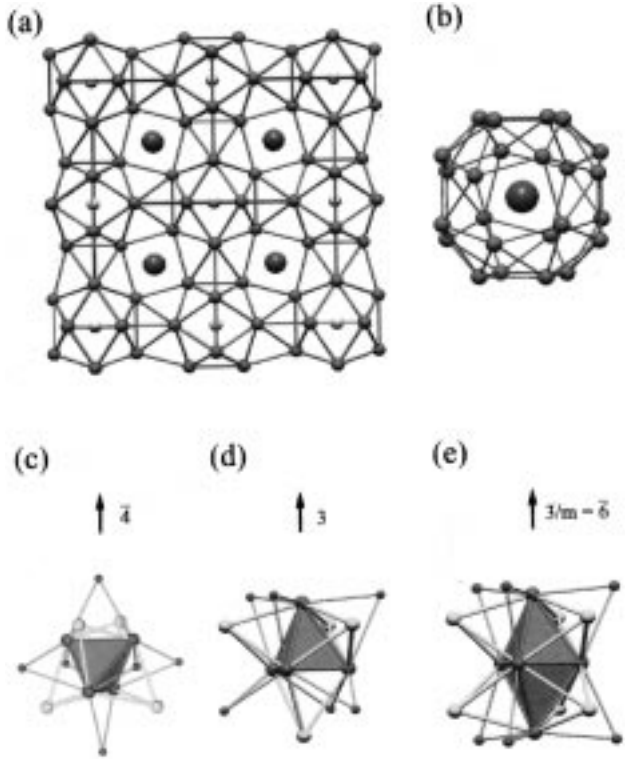

Figure 1. (a) A section of the $NaZn_{13}$ structure showing the CsCl type arrangement of centered icosahedra [Zn_{13}] and Na atoms (green circles). (b) The 24 atom snub cube coordination of a Na atom in $NaZn_{13}$. For the color graphics the program COLTURE[50] was used. (c) The cluster unit tetrahedral star (TS) oriented along the $\bar{4}$ axis and along the 3 axis (d). (e) The cluster unit double tetrahedral star (DTS) oriented along the $\bar{6}$ axis. Type T atoms are drawn as red, type C atoms as yellow, and additionally coordinating type D atoms as green circles. The central polyhedron is displayed in blue. This color code is kept in the following figures.

(13) Wangbo, M. H.; Evain; M.; Hughbanks, T.; Kertesz, M.; Wijeyesekera, S.; Wilker, C.; Zheng, C.; Hoffmann, R. *Pogram EHMACC: Extended Hückel Molecular and Crystal Calculations; Program EHPC: Extended Hückel Property Calculations*; QCPE Version, 1987.

(14) (a) Pettifor, D. G. *J. Phys. C: Solid State Phys.* **1986**, *19*, 285. (b) Pettifor, D. G.; Podloucky, R. *J. Phys. C: Solid State Phys.* **1986**, *19*, 315.

(15) (a) Lee, S. *Acc. Chem. Res.* **1991**, *24*, 249. (b) Lee S. *J. Am. Chem. Soc.* **1991**, *113*, 101. (c) Lee, S.; Rousseau, R.; Wells, C. *Phys. Rev. B* **1992**, *46*, 12121.

(16) Häussermann, U.; Nesper, R. *J. Alloys Compd.* **1995**, 218, 244.

(17) Cressoni, J. C.; Pettifor, D. G. *J. Phys.: Condens. Matter* **1991**, *3*, 495.

(18) Shoemaker, D. P.; Marsh, R. E.; Ewing, F. J.; Pauling, L. *Acta Crystallogr.* **1952**, *5*, 637.

(19) Villars, P.; Calvert, L. D. *Pearsons Handbook of Crystallographic Data for Intermetallic Compounds, Sec. Ed.*; ASM International: Materials Park, OH, 1991.

(20) Sarteschniuk, O. Z.; Kripyakevich, P. I. *Kristallografia* **1967**, *12*, 512.

(21) Nordell, K. J.; Miller, G. J. *Croat. Chim. Acta* **1995**, *68*, 825.

(22) Nyman, H.; Andersson, S. *Acta Crystallogr.* **1979** *A35*, 934.

Table 4. Selected Atomic Distances (Å) in $BaLi_7Al_6$

Ba−M2	3.797(1) × 24
M1−M2	2.732(2) × 12
M2−M2	2.812(3) × 4
M2−M2	2.851(2) × 4
M2−M2	2.962(4) × 1

of its large size in an $[Li,Al]_{13}$ framework the snub cube does probably not provide an appropriate coordination for the smaller Sr atoms, which would explain the failure of our attempts at synthesizing an isostructural compound $SrLi_7Al_6$.

4. The Basis Clusters Tetrahedral Star and Double Tetrahedral Star

An alternative description of $NaZn_{13}$ given by Nyman and Andersson starts with a partitioning of the icosahedral framework into smaller basis clusters[22] and is outlined in section 5.1.2. The cluster unit used (Figure 1c,d) consists of a central regular tetrahedron (formed by type T atoms) with all faces capped (by type C atoms). This corresponds to an arrangement of four regular tetrahedra linked facially to a central one and the point group symmetry is $\bar{4}3m$ (T_d).[23] In the literature the expressions *stella quadrangula*[24] and tetrahedral star (after *Tetraederstern*[25]) are used for this entity. In the following we refer to it as tetrahedral star (**TS**). Nyman and Andersson established TS as a valuable building unit for the description of numerous inorganic structure types. Ionic as well as intermetallic compounds are covered, ranging from subunits in Rh_7Mg_{44}[26] to extended frameworks in W_3Fe_3C,[27] Th_6Mn_{23}, γ-brass,[28] SiF_4, $CaWO_4$, $NaZn_{13}$, Ru_7B_3,[22] Tl_3VS_4, and NaPb.[29] Sometimes TS units are not linked directly via T or C atoms, but a third type of atom is introduced, bridging the edges of the central tetrahedron (type D atoms).

During our investigations of electron poor sp-bonded intermetallics we found more examples of TS based frameworks and realized that for this class of compounds the TS cluster unit is not merely a geometrical building unit but is also of electronic significance.[11] Further, we identified a second, corresponding, cluster unit named double tetrahedral star (**DTS**). The DTS ensemble (Figure 1e) consists of a trigonal bipyramid as the central polyhedron with all faces capped and has point group symmetry $\bar{6}m2$ (D_{3h}). Possible D atoms only bridge edges between equatorial and axial T atoms. In Table 5 the idealized coordinates of both cluster units are given. Characteristically, the linkage of TS and DTS units results in high-symmetry arrangements (preferably with cubic, hexagonal, or rhombohedral symmetry) which are densely packed but allow the formation of large voids. In sp-bonded intermetallics such voids are occupied by large-sized counteratoms or clusters of counteratoms from the A, Ae, or R group. In the following two sections we present examples of TS/DTS based frameworks in sp-bonded intermetallic compounds and discuss the influence of VEC on their structural stability.

Table 5. Coordinates of TS and DTS

	TS			DTS		
	x	*y*	*z*	*x*	*y*	*z*
T	0	0	*b*	0	0	±*b*
	0	*a*	0	0	*a*	0
	−1/2	−*a*/2	0	−1/2	−*a*/2	0
	1/2	−*a*/2	0	1/2	−*a*/2	0
C	5/6	5*a*/6	2*b*/3	5/6	5*a*/6	2*b*/3
	−5/6	5*a*/6	2*b*/3	−5/6	5*a*/6	2*b*/3
	0	−5*a*/3	2*b*/3	0	−5*a*/3	2*b*/3
	0	0	−*b*	5/6	5*a*/6	−2*b*/3
				−5/6	5*a*/6	−2*b*/3
				0	−5*a*/3	−2*b*/3
D	0	*d*	*e*	0	*d*	*e*
	c	−*d*/2	*e*	*c*	−*d*/2	*e*
	−*c*	−*d*/2	*e*	−*c*	−*d*/2	*e*
	0	−*d*	−1/2	0	*d*	−*e*
	c	*d*/2	−1/2	*c*	−*d*/2	−*e*
	−*c*	*d*/2	−1/2	−*c*	−*d*/2	−*e*

[a] $a = \sqrt{3}/3$; $b = \sqrt{6}/3$; $c = 1/4 + \sqrt{3/8}$; $d = 1/\sqrt{2} + 1/\sqrt{12}$; $e = 1/\sqrt{6} + 1/2$.

5. Examples of Frameworks based on Tetrahedral Stars and Double Tetrahedral Stars

5.1. Tetrahedral Star Structures. 5.1.1. NaBa. When TS units are distributed like carbon atoms in the diamond structure and connected via shared type C atoms, the Na framework of NaBa[30] ($Fd\bar{3}m$) is obtained (Figure 2a). This framework is the most open one realizable by linked TS units. In NaBa it is interpenetrated by a Ba substructure which consists of face sharing octahedra. The NaBa structure is isotypic to the [FeW] substructure in Fe_3W_3C where the TS framework of Fe atoms was recognized by Nyman et al.[27]

Proceeding with the same kind of linkage, a much denser TS framework is obtained when the TS units are arranged in an fcc manner, and type C atoms are shared between four clusters (Figure 2b). In the idealized structure the intercluster distances (between T atoms) are shorter than the distances within the TS unit and voids for hosting more electropositve counteratoms are not present. The framework is not observed as a three-dimensional structure, but parts of it reveal an intriguing structural coincidence to a 29 atom cluster unit found in the structures of β-rhombohedral boron and some related (more electron rich) A/E12/Tr polar intermetallics (e.g., $K_{34}[Zn_{20}In_{85}]$,[8] $Na_{17}[Zn_{12}Ga_{40.5}]$,[31] $Na_{17}[Cu_6Ga_{46.5}]$[32]). Figure 2c shows an ensemble of seven TS units in a closed-packed layer. If we remove all atoms outside the black line drawn and all (type C) atoms but the central one from the layer *a* and take further into account the atoms from layer *e*, icosahedral fragments emerge (Figure 2d). The final 29 atom arrangement is completed by small "relaxation" movements and the insertion of three additional atoms as indicated in Figure 2d. It corresponds to a TS linking together three slightly distorted icosahedra, and these icosahedra appear face condensed (Figure 2e). In β-rhombohedral boron and related structures such cluster units are embedded in a matrix of exo-bonded icosahedra.

5.1.2. SiF_4 and $NaZn_{13}$. In the structure of SiF_4,[33] ($I\bar{4}3m$) F atoms form a bcc arrangement of TS. The basis clusters are corner-connected in such a way that a type C atom corresponds to a type T atom in the neighboring cluster and vice versa (Figure 3a). This particular arrangement creates a void defined by eight atoms resembling a distorted dodecahedron (bisdis-

(23) Note, that there exists a distorted variant of TS with point group symmetry $42m$ (D_{2d}). This kind of cluster is not considered here.

(24) Hyde, B. G.; Andersson, S. *Inorganic Crystal Structures*; John Wiley & Sons: New York, 1989.
(25) Schubert, K. *Kristallstrukturen zweikomponentiger Systeme*; Springer: Berlin, 1964; p. 150 (in German).
(26) Andersson, S. *Acta Crystallogr.* **1978**, *A34*, 833.
(27) Nyman, H.; Andersson, S.; Hyde, B. G.; O'Keeffe, M. *J. Solid State Chem.* **1978**, *26*, 123.
(28) Nyman, H.; Andersson, S. *Acta Crystallogr.* **1979**, *A35*, 580.
(29) Nyman, H. *Acta Crystallogr.* **1983**, *B39*, 529.
(30) Snyder, G. J.; Simon, A. *J. Chem. Soc., Dalton Trans.* **1994**, 1159.
(31) Tillard-Charbonell, M.; Chouaibi, N.; Belin, C. *R. Acad. Sci. Paris* **1992**, *315*, 661.
(32) Tillard-Charbonell, M.; Chouaibi, N.; Lapasset, J.; Belin, C. *J. Solid State Chem.* **1992**, *100*, 220.
(33) Atoji, M.; Lipscomb, W. N. *Acta Crystallogr.* **1954**, *7*, 597.

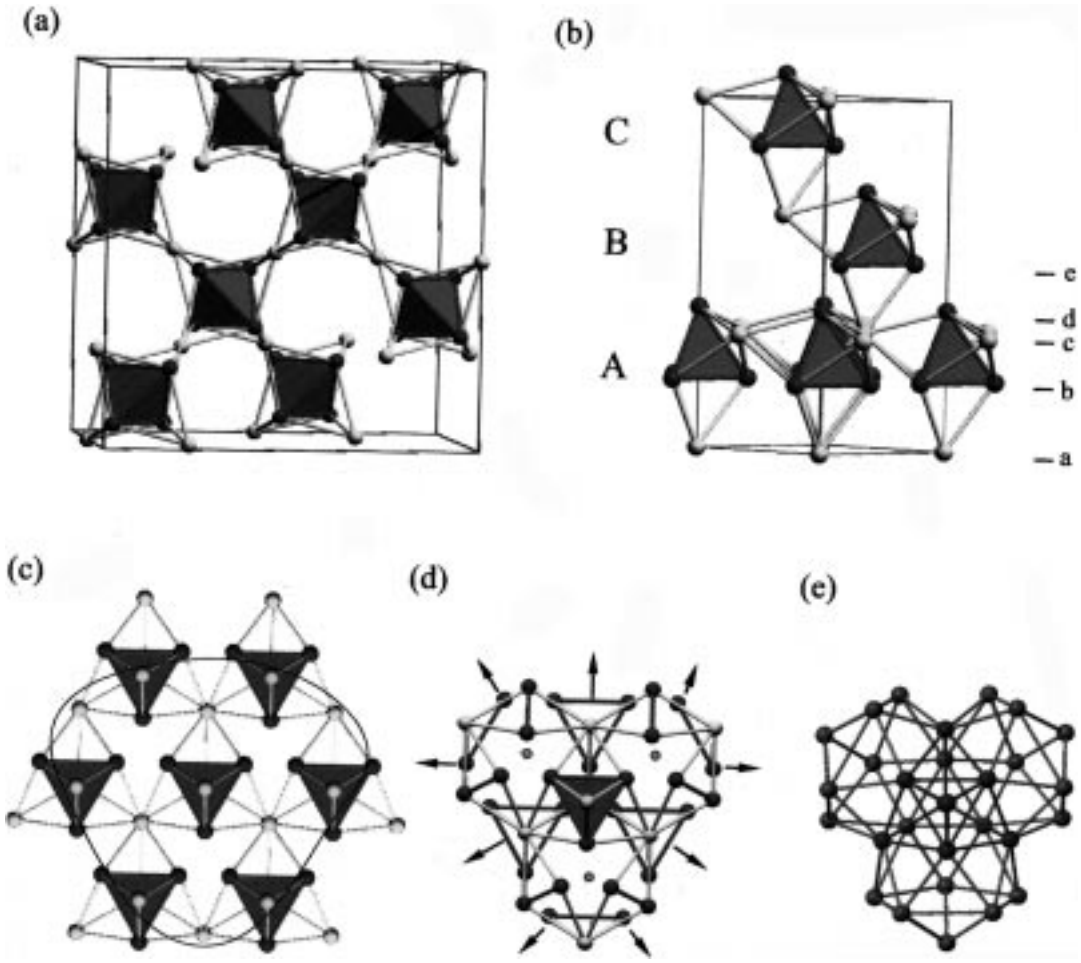

Figure 2. (a) The TS framework formed by the Na atoms in NaBa. (b) A hypothetical framework with fcc arranged TS clusters sharing type C atoms. (c) A section of a closed-packed layer of TS units (atomic layers $a-d$ in Figure 2a). When removing the atoms outside the black line and adding those from atomic layer e an ensemble (d) is obtained which can easily be distorted and completed to a cluster unit found in β-rhombohedral boron. (e) The 29 atom cluster in β-rhombohedral boron: a TS unit condensing three icosahedra.

phenoid) (Figure 3b). A hypothetical compound with these voids occupied by (large) atoms X would have the composition X_3Z_4 but is not known. Apparently this kind of TS arrangement is only stable for ionic compounds where additionally the central tetrahedron of the TS is centered by a small, highly polarizing cation.

Surprisingly, exactly the same kind of TS linkage is found in the structure of $NaZn_{13}$ (Figure 3c), and the—at the first sight so different—TS frameworks of SiF_4 and $NaZn_{13}$ appear as "isomeres". Whereas in SiF_4 all TS units have the same orientation, they are mutually rotated in $NaZn_{13}$. This yields a less dense TS packing for $NaZn_{13}$ and the formation of two different kinds of (larger) voids. In $NaZn_{13}$ 12 out of the 13 Zn atoms of a formula unit participate in the TS framework. The first void corresponds to the center of an icosahedron (Figure 3d) and is occupied by the remaining Zn atom. The second void is defined by 24 Zn atoms of the TS framework and hosts the Na atoms (cf. Figures 1a, b, and 3c). The description of the $NaZn_{13}$ structure based on TS units accounts elegantly for the formation of the icosahedra *and* their linkage and was presented by Nyman and Andersson.[22] It is important to note that the TS framework in $NaZn_{13}$ can only be built from slightly distorted TS.

5.1.3. Th_6Mn_{23} and $Ba_2Li_{4.21}Al_{4.79}$. In the cubic Th_6Mn_{23} structure[34] ($Fd\bar{3}m$) TS units are connected via type D atoms in such a way that one D atom belong to two TS clusters, and the resulting three-dimensional array of clusters is of the simple cubic type. This structural description has already been made by Nyman and Andersson.[28] However, for comparing the Th_6Mn_{23} structure with related ones the rhombohedral representation is preferable. In this representation the building block of the TS framework consists of two connected layers of hexagonally arranged TS units (Figure 4a). It is important to note that the two layers of such a double layer are inversely orientated. The complete TS framework, which includes 22 atoms out of 23 Mn atoms of a formula unit, is obtained by stacking the double layers in an ABC sequence and connecting them via the type D atoms. The large voids within a double layer are occupied by Th_6 octahedra, and the smaller voids between two double layers introduced by the stacking are occupied by the remaining Mn atoms (Figure 4b).

The structure of $Ba_2Li_{4.21}Al_{4.79}$[11] ($R\bar{3}m$) can simply be obtained from the Th_6Mn_{23} structure by shearing the two TS layers of a double layer until the type C atoms of two TS units meet (shift vectors (1/3, 2/3, 0) or (2/3, 1/3, 0)) (Figure 4c). Now the TS units within a double layer are connected via shared type C atoms and the resulting ensembles represent centered icoshedral units, but the stacking and linkage of the double layers is analogous to the Th_6Mn_{23} structure (Figure 4d). In $Ba_2Li_{4.21}Al_{4.79}$ eight out of the nine atoms of the (Li,Al) majority component participate in the TS framework.

(34) Florio, J.; Rundle, R. E.; Snow, I. A. *Acta Crystallogr.* **1952**, *5*, 449.

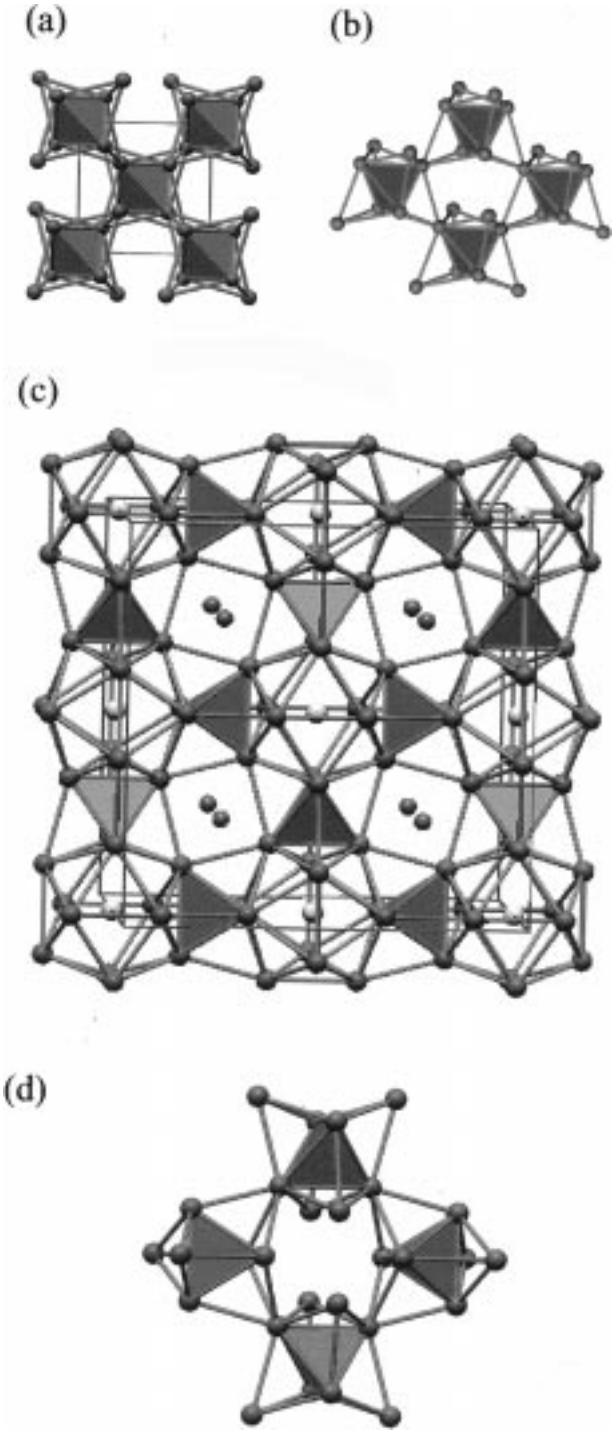

Figure 3. (a) The TS arrangement in the structure of SiF_4 ($I\bar{4}3m$). (b) The void defined by eight atoms is centered at the position 6b (0, 1/2, 1/2). Note, that in SiF_4 actually six TS units are situated around this position. (c) The isomeric TS arrangement in the structure of $NaZn_{13}$ ($Fm\bar{3}c$). Here and in the following figures, atoms of the majority component not participating in a TS/DTS framework are drawn as white circles, the more electropositive counteratoms as black circles. (d) The void defined by 12 atoms is centered at position 8b (0, 0, 0). Note, that in $NaZn_{13}$ actually six TS units are situated around this position which is occupied by the additional Zn atoms.

5.1.4. $BaHg_{11}$ and $Cr_{23}C_6$. In the cubic $BaHg_{11}$ structure[35] (*Pm*3*m*) eight TS units form a supercluster. Figure 5a,b shows the connectivity. Three of the four type T atoms of a TS unit are shared between neighboring TS units, and all eight TS units share a common type C atom located at the center of the supercluster (and the unit cell). The supercluster consists of 20 T and 25 C atoms and describes all atomic positions of the majority component in $BaHg_{11}$ (Figure 5c). In the three-dimensional structure superclusters are connected via common type C atoms located at the faces of the unit cell which yields a simple cubic arrangement (cf. Figure 5c) with large voids defined by 20 atoms. The voids are centered by the Ba atoms. When building the TS framework in $BaHg_{11}$ from idealized TS units the distance between the supercluster linking type C atoms becomes rather short.

The TS framework of $Cr_{23}C_6$[36] (*Fm*3*m*) is obtained when the TS superclusters of $BaHg_{11}$ are connected in a fcc type manner instead of the sc arrangement in $BaHg_{11}$ (Figure 5d). This kind of linkage is only possible with slightly distorted TS units and excludes the formation of large voids.

5.1.5. $BaCd_{11}$ and β-Mn. The central building unit of the tetragonal $BaCd_{11}$ structure[37] ($I4_1/amd$) is a TS strand in which the central tetrahedra of the basis clusters share edges. Figure 6a depicts the connectivity. Each type T atom belongs to two TS units and is at the same time a type C atom in the neighboring cluster and vice versa. The remaining type C atoms (yellow spheres in Figure 6a) are also shared between two units. This strand cannot be built from ideal TS. Its translational period consists of four units (Figure 6b), and the translational direction coincides with a 4_1 or a 4_3 axis. Figure 6c shows the projection along this direction. The unit cell of $BaCd_{11}$ contains four tetragonally arranged TS strands which are linked by shared type C atoms (Figure 6d). Both kinds of strands (4_1 and 4_3 type) occur, with a 4_1 strand being surrounded and connected to four 4_3 strands and vice versa. Ten out of the 11 Cd atoms of a formula unit participate in this TS framework which possesses two different kinds of voids alternately arranged in the *c* direction. The smaller void (defined by 12 TS atoms) is occupied by the remaining Cd atoms, the larger void (defined by 16 TS atoms) by the Ba atoms.

Intriguingly the cubic β-Mn structure[38] ($P4_332$ or the enantiomorphous $P4_132$) can be constructed from the same kind of TS strands analogously linked together as in $BaCd_{11}$. Figure 6e depicts a (100) projection of the β-Mn structure. The chiral TS framework consists of 4_3 strands in two different orientations, tilted by $\approx 6°$ and $\approx -6°$, respectively, away from the unit cell axes. The angle between two linked TS strands, as defined in Figure 6e, is $\approx 102°$. Rotating the strands until the angle between them becomes 180° (sketched in Figure 6e) yields a TS framework topologically equivalent to that in the $BaCd_{11}$ structure. The sole difference is that the expanded β-Mn framework contains only one kind of TS strand (either type 4_1 or 4_3).[39]

5.2. Double Tetrahedral Star Structures. 5.2.1. $Ba_3Li_3Ga_{4.1}$. When linking DTS units in such a way that two clusters share type C atoms corresponding to the linkage of the TS units in NaBa, one can think of two possible high-symmetrical hexagonal arrangements (Figure 7a). In the first framework each DTS unit is connected to six other units which surround the central cluster in a trigonal prismatic way. The three-dimensional framework can be described in terms of (connected) α-arsenic type layers of DTS clusters which are

(35) Peyronel, G. *Struct. Rep.* **1952**, *16*, 24.

(36) Bowman, A. L.; Arnold, G. P.; Storms, E. K.; Nereson, N. G. *Acta Crystallogr.* **1972**, *B28*, 3102.

(37) Sanderson, M. J.; Baenziger, N. C. *Acta Crystallogr.* **1953**, *6*, 627.

(38) Shoemaker, C. B.; Shoemaker, D. P.; Hopkins, T. E.; Yindepit, S. *Acta Crystallogr.* **1978**, *B34*, 3573.

(39) A related description of the β-Mn structure based on helices of face-sharing tetrahedra has been given by Nyman, H.; Carroll, C. E.; Hyde, B. G. *Z. Kristallogr.* **1991**, *196*, 39.

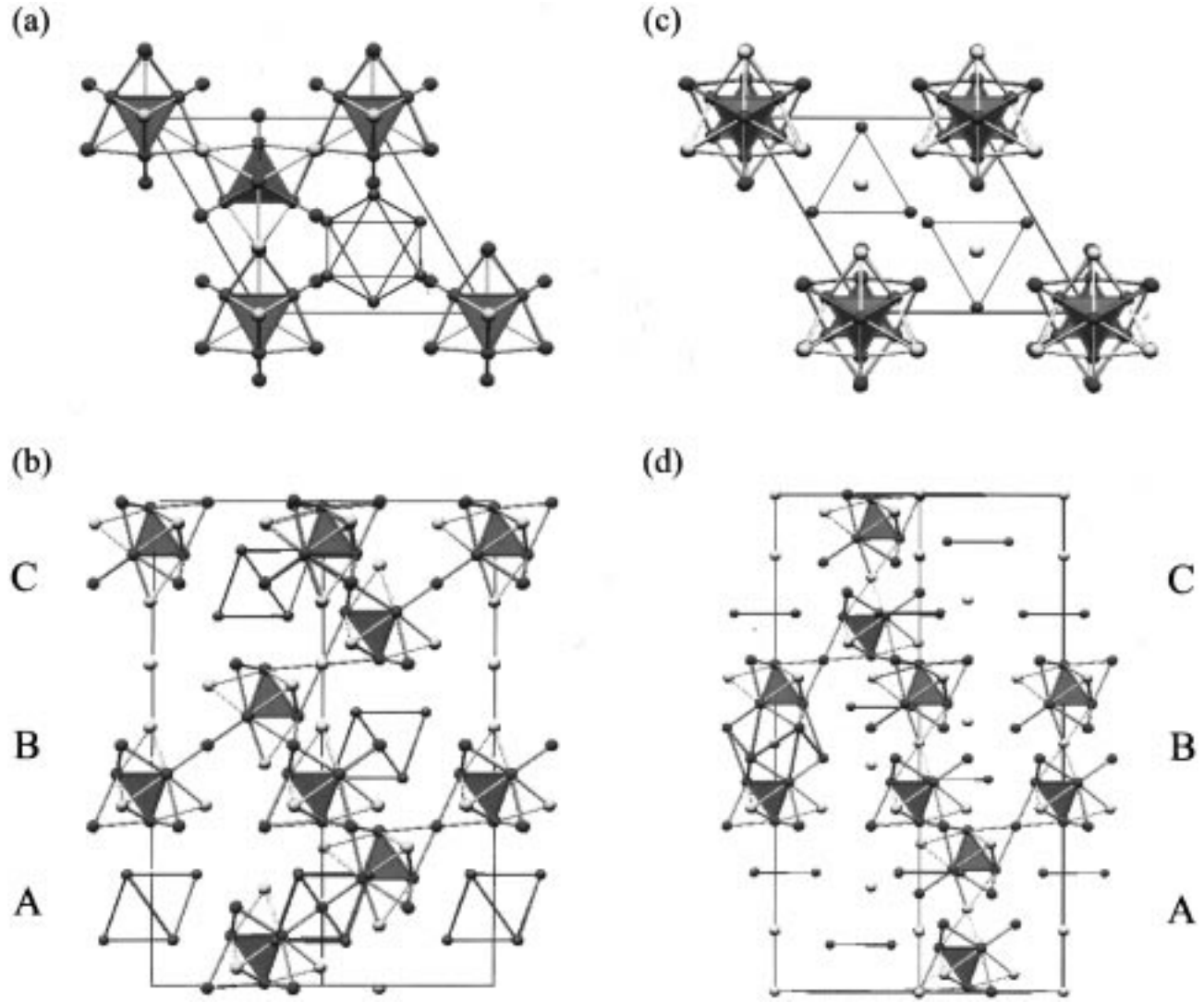

Figure 4. (a) A double layer consisting of two layers of hexagonally arranged TS units in Th_6Mn_{23}. The TS clusters are connected via type D atoms. (b) ABC stacking of such double layers in the complete structure of Th_6Mn_{23} (projection along [11$\bar{2}$0], rhombohedral representation). (c) A double layer of TS units in $Ba_2Li_{4.21}Al_{4.79}$. Compared to the double layer in Th_6Mn_{23} the TS units are connected via common type C atoms. (d) ABC stacking of such double layers in the complete structure of $Ba_2Li_{4.21}Al_{4.79}$ (projection along [11$\bar{2}$0]). One icosahedra formed by two, via type C atom condensed and type D atom coordinated, TS units is outlined.

AA stacked in the *c* direction. The distance between axial T atoms of DTS units situated on top of each other becomes very short in the idealized framework compared to the distances within the DTS units (Figure 7b). In the second framework each DTS unit is linked to only three other clusters which share two type C atoms each with the central one. This linkage leads to isolated graphite type layers of DTS units which might be stacked in any sequence (Figure 7c). In the case of an AA stacking the (001) projections of the two kinds of DTS frameworks look alike (Figure 7a).

The first kind of framework seems to be realized in the recently discovered compound $Ba_3Li_3Ga_{4.1}$[40] ($P6_3/mc$). Ga atoms occupy the positions of the T atoms and Li atoms those of the C atoms. The large channels along the unit cell *c* axis host strands of face condensed empty Ba octahedra (Figure 7a,b). In this structure the central trigonal bipyramids are considerably contracted which lengthens the short distances between the axial T atoms of DTS units situated on top of each other. Additionally, the positions of these axial type T atoms are only partly occupied—in a remarkably unsymmetrical way which destroys the centrosymmetry of the structure. Thus, it was also speculated that the central polyhedron of the cluster unit could actually be a tetrahedron and the structure a twin.[40]

The second kind of framework is not yet known as a three-dimensional structure, but the arrangement of DTS units in a single graphite type layer is found as a structural motif in the more electron rich polar intermetallics $A_{15}Tl_{27}$ (A = Rb, Cs)[41] and $K_{14}Cd_9Tl_{21}$.[42] In both structures the DTS units are mutually rotated compared to the high-symmetrical arrangement in Figure 7c. This distroys the 6/*m* axis and diminishes the size of the void.

5.2.2. $BaLi_4$ and $CaZn_3$. In the hexagonal structure of $BaLi_4$[43] ($P6_3/mmc$) DTS units form rods along the c direction by sharing the axial type T atoms (Figure 7d). In such rods DTS units are alternately rotated by 180° yielding icosahedral units, and the rod can be equivalently described as a linear chain

(40) Hofmann, P. Ph.D. Thesis; ETH Zürich: Zürich, Switzerland, 1997.

(41) Dong, Z.; Corbett, J. D. *Inorg. Chem.* **1996**, *35*, 1444.

(42) (a) Tillard-Charbonell, M.; Chahine, A.; Belin, C. *Z. Kristallogr.* **1995**, *210*, 162. (b) Tillard-Charbonell, M.; Chahine, A.; Belin, C.; Rousseau, R.; Canadell, E. *Chem. Eur. J.* **1997**, *3*, 799.

(43) Kanda, F. A.; Miskell, C. F.; King, A. J. *Acta Crystallogr.* **1965**, *18*, 24.

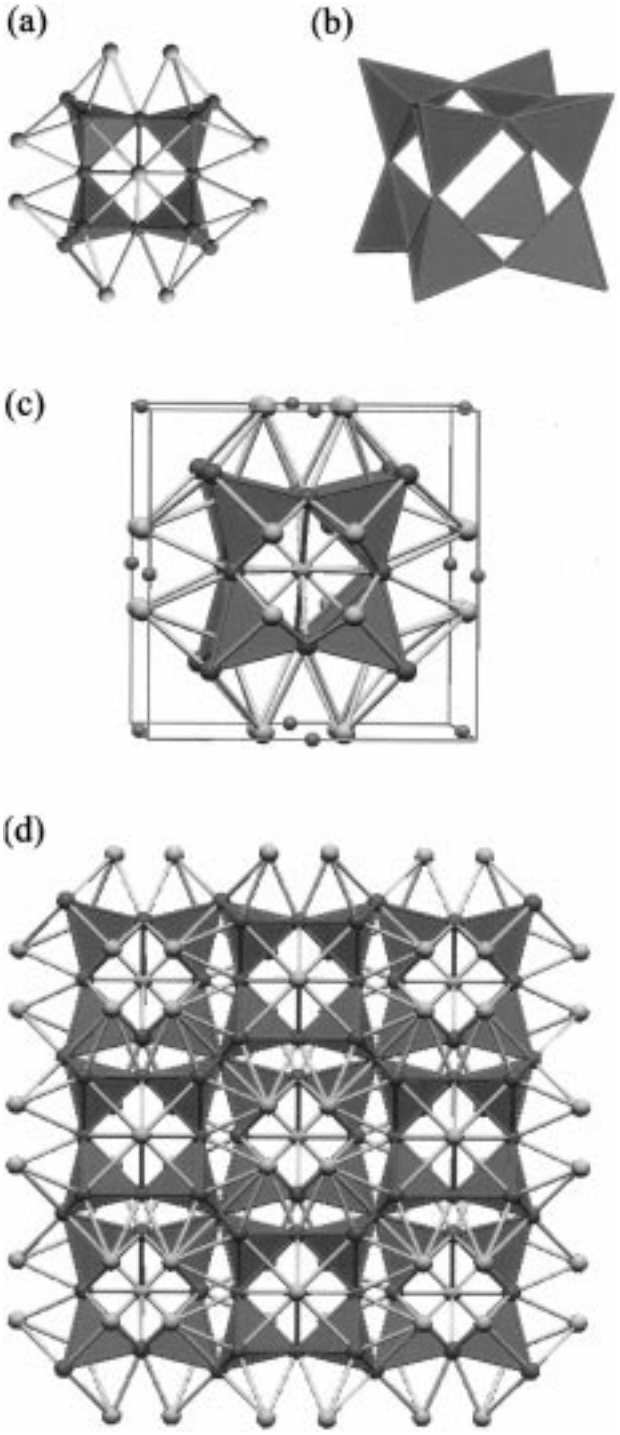

Figure 5. (a) One half of the supercluster formed by TS units in $BaHg_{11}$. (b) The arrangement of the central tetrahedra in the complete, eight TS units containing, supercluster. (c) View of the unit cell for $BaHg_{11}$. (d) Arrangement of the superclusters in the structure of $Cr_{23}C_6$.

of face condensed centred icosahedra (Figure 7e). In $BaLi_4$ the rods are not connected directly to each other but via interstitial Li atoms. These interstitial atoms between the rods represent 1/4 of the Li atoms in $BaLi_4$ and are arranged alternately with triangular Ba units along the *c* direction (Figure 7e). The related DTS framework with directly linked rods (*P*6/*mmm*), as displayed in Figure 7f, has not been observed yet. An appropriate compound with the large voids centered at (0,0,0) and (0,0,1/2) occupied by X atoms would have the composition XZ_{17}.

The $CaZn_3$ structure[44] is a variation of the $BaLi_4$ structure. Besides the Ca atoms corresponding to the Ba atoms in $BaLi_4$, additional Ca atoms center partly the central trigonal bipyramid of the DTS units. These positions are not fully occupied.

5.2.3. $EuMg_{5.2}$ and $ErZn_5$. The DTS framework of the hexagonal $EuMg_{5.2}$[45] and $ErZn_5$[46] structures (*P*6$_3$/*mmc*) corresponds to the TS framework of Th_6Mn_{23}: hexagonally arranged layers of DTS units are stacked in an AB sequence and linked via shared type D atoms (Figure 8a,b). (Note that the AB sequence is a consequence of this kind of linking.) Large voids within the DTS layers host triangular R atom clusters. and the composition of such an arrangement is X_3Z_{14}. The channels along the unit cell *c* axis introduced by the stacking are occupied by the remaining small fraction of majority component atoms. In $EuMg_{5.2}$ Mg atoms are distributed in a disordered way along this axis, wheras in $ErZn_5$ the position (0,0,1/4) is fully occupied.

5.3. Structures Containing Both Kinds of Clusters. Sr_3Mg_{13} and $Sr_9Li_{17.5}Al_{25.5}$. The hexagonal structure of Sr_3Mg_{13}[45] (*P*6$_3$/*mmc*) shown in Figure 8c is a perfect intergrowth of the $ErZn_5$ and the Th_6Mn_{23} structure (cf. Figures 8b and 4b). The TS/DTS framework includes 12 out of the 13 Mg atoms of a formula unit.

When applying the (icosahedra-forming) shear operation driving the transformation $Th_6Mn_{23} \rightarrow Ba_2Li_{4.21}Al_{4.79}$ (section 5.1.3, Figure 4c) to the TS double layers in Sr_3Mg_{13}, the $Sr_9Li_{17.5}Al_{25.5}$ structure is obtained (Figure 8d).[11] In $Sr_9Li_{17.5}Al_{25.5}$ 36 out of the 43 atoms of the (Li,Al) majority component form the TS/DTS framwork. The relationship between the structures of Th_6Mn_{23}, Sr_3Mg_{13}, $EuMg_{5.2}$, $Ba_2Li_{4.21}Al_{4.79}$, and $Sr_9Li_{17.5}Al_{25.5}$ has been described in more detail elsewhere.[11]

6. Structural Stability of the Frameworks

The presented structures of the previous section are adopted with strongly varying frequencies among known intermetallic compounds (we do not count the SiF_4 structure as an intermetallic structure type), e.g., the Th_6Mn_{23} type with several hundreds of representatives and the $Ba_2Li_{4.21}Al_{4.79}$ type with only one. The geometrical description of the frameworks formed by the majority component in terms of TS/DTS clusters appears as a valuable concept for comparing, relating, and rationalizing these rather complicated structures and includes even the possibility of predicting new ones. The cluster units are very flexible in their connectivity which affords an outstanding variability for the generation of such frameworks. TS units have to be slightly distorted in the frameworks of $NaZn_{11}$, $Cr_{23}C_6$, $BaCd_{11}$, and β-Mn in order to ensure the translational symmetry.[47] Further, we observe deviations from the idealized framworks when the kind of linkage causes short distances between atoms of neighboring cluster units, as in $BaHg_{11}$ and $Ba_3Li_3Ga_{4.1}$. In Table 6 the idealized frameworks are compared with actual structural parameters. A third reason of distortion is the formation of icosahedral aggregates from TS or DTS units, as observed for the hexagonal or rhombohedral structures of $BaLi_4$, $Ba_2Li_{4.21}Al_{4.79}$, and $Sr_9Li_{17.5}Al_{25.5}$. This distortion appears as a compression in the c direction which causes the distances between icosahedra-forming atoms to become more equal but leaving their fractional coordinates unchanged.

(44) Fornasini, M. L.; Merlo, F. *Acta Crystallogr.* **180**, *B36*, 1739.
(45) Erassme, J.; Lueken, H. *Acta Crystallogr.* **1987**, *B43*, 244.
(46) Fornasini, M. L. *J. Less-Common Met.* **1971**, *25*, 329.

(47) Concerning the distortion of TS strands: the nonperiodicity of a helix consisting of face-sharing regular tetrahedra has been analyzed by (a) Zheng, C.; Hoffmann, R.; Nelson, D. R. *J. Am. Chem. Soc.* **1990**, *112*, 3784. (b) Nyman, H.; Carroll, C. E.; Hyde, B. G. *Z. Kristallogr.* **1991**, *196*, 39. (c) Lidin, S.; Andersson, S. *Z. Anorg. Allg. Chem.* **1996**, *622*, 164.

Table 6. Comparison of the Idealized Frameworks (bold) with Actual Structural Parameters

NaBa ($Fd\bar{3}m$)									
atom	site	*x*	*y*	*z*	atom	site	*x*	*y*	*z*
T	**32e**	**0.3**	**0.3**	**0.3**	**C**	**16d**	**1/2**	**1/2**	**1/2**
		0.2946	0.2946	0.2946					
Th_6Mn_{23} ($Fm3m$)									
atom	site	*x*	*y*	*z*	atom	site	*x*	*y*	*z*
T	**32f**	**0.177526**	**0.177526**	**0.177526**	**C**	**32f**	**0.370791**	**0.370791**	**0.370791**
	Sr_6Mg_{23}	0.1774	0.1774	0.1774		Sr_6Mg_{23}	0.3741	0.3741	0.3741
	Sr_6Li_{23}	0.178	0.178	0.178		Sr_6Li_{23}	0.378	0.378	0.378
	$Ca_6Li_{12}Al_{11}$	0.1756	0.1756	0.1756		$Ca_6Li_{12}Al_{11}$	0.3763	0.3763	0.3763
	$Mg_6Cu_{16}Si_7$	0.121	0.121	0.121		$Mg_6Cu_{16}Si_7$	0.334	0.334	0.334
					D	**24d**	**0**	**1/4**	**1/4**
$Ba_2Li_{4.21}Al_{4.79}$ ($R\bar{3}m$)		***c/a* = 3.0**							
$Ba_2Li_{4.21}Al_{4.79}$		*c/a* = 2.714							
atom	site	*x*	*y*	*z*	atom	site	*x*	*y*	*z*
T1	**6c**	**0**	**0**	**0.342199**	**C1**	**18h**	**0.494388**	**0.505612**	**0.298167**
		0	0	0.3363			0.5017	0.4983	0.2999
T2	**18h**	**0.429986**	**0.570014**	**0.087766**	**C2**	**3b**	**0**	**0**	**1/2**
		0.4283	0.5717	0.0892	**D1**	**18h**	**0.5**	**0.5**	**0.197251**
							0.4905	0.5095	0.1842
					D2	**9e**	**1/2**	**0**	**0**
$BaHg_{11}$ ($Pm3m$)									
atom	site	*x*	*y*	*z*	atom	site	*x*	*y*	*z*
T1	**8g**	**0.2**	**0.2**	**0.2**	**C1**	**1b**	**0**	**0**	**0**
	$BaHg_{11}$	0.155	0.155	0.155	**C2**	**12i**	**0**	**0.375**	**0.375**
	$CaAg_4Al_7$	0.1660	0.1660	0.1660		$BaHg_{11}$	0	0.345	0.345
T2	**12j**	**1/2**	**0.275**	**0.275**		$CaAg_4Al_7$	0	0.3427	0.3427
	$BaHg_{11}$	1/2	0.275	0.275					
	CaAg4Al7	1/2	0.2654	0.2654					
$Ba_3Li_3Ga_{4.1}$ ($P6_3/mmc$)		***c/a* = 0.653197**							
$Ba_3Li_3Ga_{4.1}$ ($P6_3/mc$)		*c/a* = 0.689							
atom	site	*x*	*y*	*z*	atom	site	*x*	*y*	*z*
T^{ax}	**4e**	**1/3**	**2/3**	**0.625**	**T^{eq}**	**6h**	**0.233333**	**0.466667**	**1/4**
	2b	1/3	2/3	0.9407 (0.5593)[a]		6c	0.237	0.474	0.25
	2b	1/3	2/3	0.5616	**C**	**6g**	**1/2**	**0**	**0**
						6c	0.4985	0.997	−0.0137
$BaLi_4$ ($P6_3$/mmc)		***c/a* = 0.979796**							
$BaLi_4$		*c/a* = 0.806							
$CaZn_3$		*c/a* = 0.799							
atom	site	*x*	*y*	*z*	atom	site	*x*	*y*	*z*
T^{ax}	**2a**	**0**	**0**	**0**	**C**	**12k**	**0.166667**	**0.333333**	**0.583333**
T^{eq}	**6h**	**0.1**	**0.2**	**1/4**		$BaLi_4$	0.1621	0.3242	0.5615
	$BaLi_4$	0.1027	0.2054	1/4		$CaZn_3$	0.1692	0.3384	0.5556
	$CaZn_3$	0.0978	0.1956	1/4					
$EuMg_{5.2}$ ($P6_3/mmc$)		***c/a* = 1.053197**							
$ErZn_5$		*c/a* = 1.037							
$EuMg_{5.2}$		*c/a* = 1.034							
atom	site	*x*	*y*	*z*	atom	site	*x*	*y*	*z*
T^{ax}	**4f**	**1/3**	**2/3**	**0.025255**	**C**	**12k**	**0.172279**	**0.344558**	**0.100170**
	$ErZn_5$	1/3	2/3	0.0054		$ErZn_5$	0.1728	0.3457	0.0904
	$EuMg_{5.2}$	1/3	2/3	0.9981		$EuMg_{5.2}$	0.1599	0.3192	0.0888
T^{eq}	**6h**	**0.429966**	**0.859932**	**1/4**	**D**	**6g**	**1/2**	**0**	**0**
	$ErZn_5$	0.4318	0.8636	1/4					
	$EuMg_{5.2}$	0.4320	0.8640	1/4					
Sr_3Mg_{13} ($P6_3/mmc$)		***c/a* = 2.686190**							
Sr_3Mg_{13}		*c/a* = 2.691							
atom	site	*x*	*y*	*z*	atom	site	*x*	*y*	*z*
T1	**4f**	**1/3**	**2/3**	**0.642078**	**C1**	**4f**	**1/3**	**2/3**	**0.034157**
		1/3	2/3	0.6491			1/3	2/3	0.0375
T2	**12k**	**0.236701**	**0.473402**	**0.553961**	**C2**	**12k**	**0.494388**	**0.988776**	**0.612706**
		0.2323	0.4646	0.5545			0.5034	0.0068	0.6179
T^{ax}	**4e**	**0**	**0**	**0.161882**	**C3**	**12k**	**0.161054**	**0.322109**	**0.191255**
		0	0	0.1582			0.1757	0.3514	0.1902
T^{eq}	**6h**	**0.903367**	**0.806735**	**1/4**	**D1**	**6g**	**1/2**	**0**	**0**
		0.9012	0.8024	1/4	**D2**	**12k**	**0.166667**	**0.333333**	**0.651980**
							0.1669	0.3338	0.6536

Table 6. (Continued)

$Sr_9Li_{17.5}Al_{25.5}$ ($P6_3/mmc$) **$c/a = 3.053197$**									
$Sr_9Li_{17.5}Al_{25.5}$		$c/a = 2.962$							
atom	site	*x*	*y*	*z*	atom	site	*x*	*y*	*z*
T1	**4e**	**0**	**0**	**0.155051**	**C1**	**12k**	**0.494388**	**0.988776**	**0.698316**
		0	0	0.1589			0.5012	0.0024	0.6940
T2	**12k**	**0.096633**	**0.193266**	**0.577526**	**C2**	**12k**	**0.161054**	**0.322109**	**0.129209**
		0.0969	0.1938	0.5750			0.1696	0.339	0.1290
T^{ax}	**4f**	**1/3**	**2/3**	**0.672474**	**C3**	**2a**	**0**	**0**	**0**
		1/3	2/3	0.6657	**D1**	**12k**	**0.166667**	**0.333333**	**0.030057**
T^{eq}	**6h**	**0.763299**	**0.526598**	**1/4**			0.1623	0.3247	0.0169
		0.7633	0.5267	1/4	**D2**	**12k**	**0.166667**	**0.333333**	**0.663763**
							0.1682	0.3365	0.6621

[a] In noncentrosymmetric $Ba_3Li_3Ga_{4.1}$ the T^{ax} atoms are distributed on two different sites. The *z* parameter in parentheses is the corresponding "centrosymmetric" value for this position.

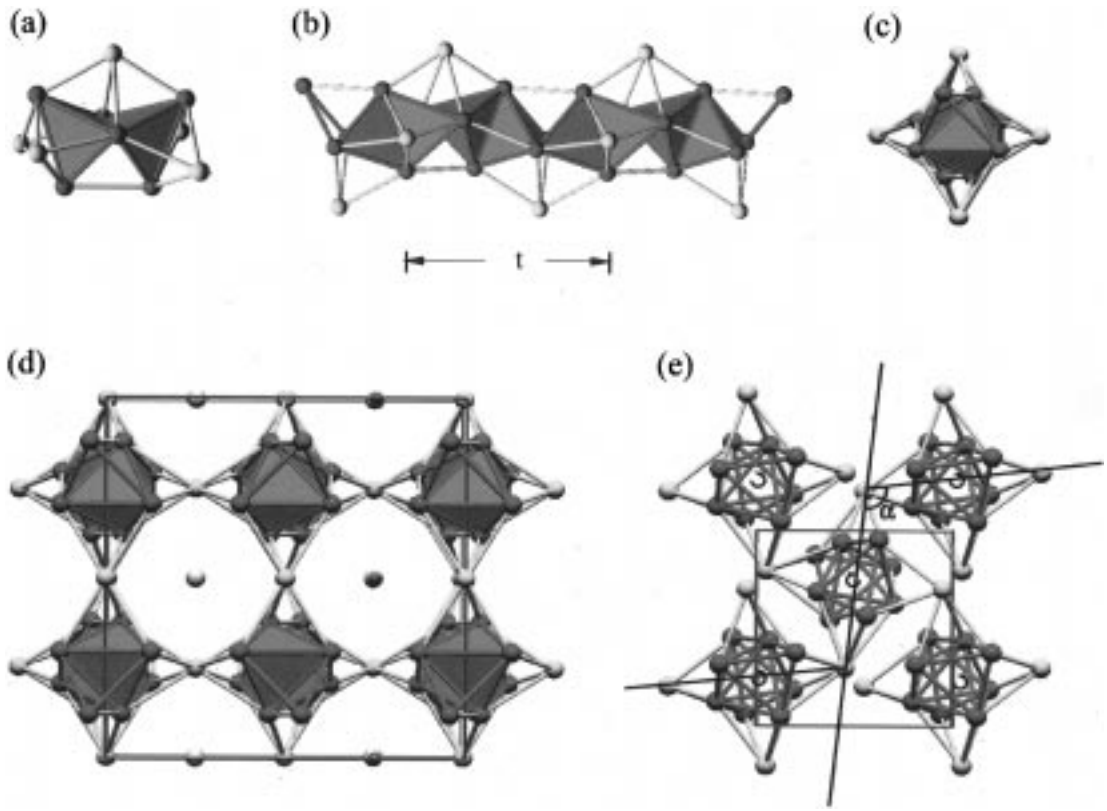

Figure 6. (a) Two (slightly distorted) TS units connected via common edges. (b) A strand of edge-connected (slightly distorted) TS units. The repetition unit contains four entities. (c) Projection of the strand along the translational direction. (d) The arrangement of the TS strands in $BaCd_{11}$ ((001) projection). (e) The arrangement of the TS strands in β-Mn. The angle α between two TS strands is $\approx$102°. By a rotation of the strands in the directions indicated, a framework topologically equivalent to that in $BaCd_{11}$ is obtained when $\alpha = 180°$.

We now turn to the question of the electronic significance of the TS/DTS concept by investigating the influence of VEC on the structural stability of the presented frameworks. We are particularly interested in sp-bonded compounds and the inspection of Pearson's Handbook of Crystallographic Data for Intermetallic Phases[19] for the appropriate representatives of the presented structure types confirms the observation already made in connection with the $NaZn_{13}$ structure type (section 3): in binary compounds the majority component is basically one of the divalent metals of highest electronegativity Be, Mg, Zn, Cd, or Hg with large A, Ae, or R atoms as counterparts. In ternary compounds the divalent majority component is replaced by combinations Li/Al, Cu/Al, Ag/Al and less frequently by Cu/In, Cu/Ga, and Li/Ga. We try to answer our key question: Can this family of intermetallic compounds be understood in the spirit of the Zintl−Klemm concept, i.e., is the framework formally reduced by the electropositive component in order to adopt an optimum VEC? For answering this question we calculated stability curves for the particular framework structures with the simple TB binding Hückel method. A stability curve represents the electronic energy difference between framework and a reference structure as a function of VEC (section 2.3).[48] The maximum values of such a stability curve inidicate the regions of VEC a framework should adopt for maximum structural stability. The values obtained for the different frameworks can be compared to each other.[49] However, it remains difficult to compare amplitudes of stability curves of different substructures in order to make predictions about structural competition. Each framework is stabilized by the interaction with the more electropositive counteratoms, and this

(48) (a) J. K. Burdett, S. Lee, *J. Am. Chem. Soc.* **1985**, *107*, 3050. (b) J. K. Burdett, S. Lee, *J. Am. Chem. Soc.* **1985**, *107*, 3063.

(49) The maximum values of the stability curves are only very slightly affected by the choice of the second moment (see section 2.3). When calculating stability curves using the extreme values of this quantity corresponding to fcc-Al and the Al framework in $BaAl_4$, the maximum positions differed by not more than 0.1 e/atom for most of the frameworks.

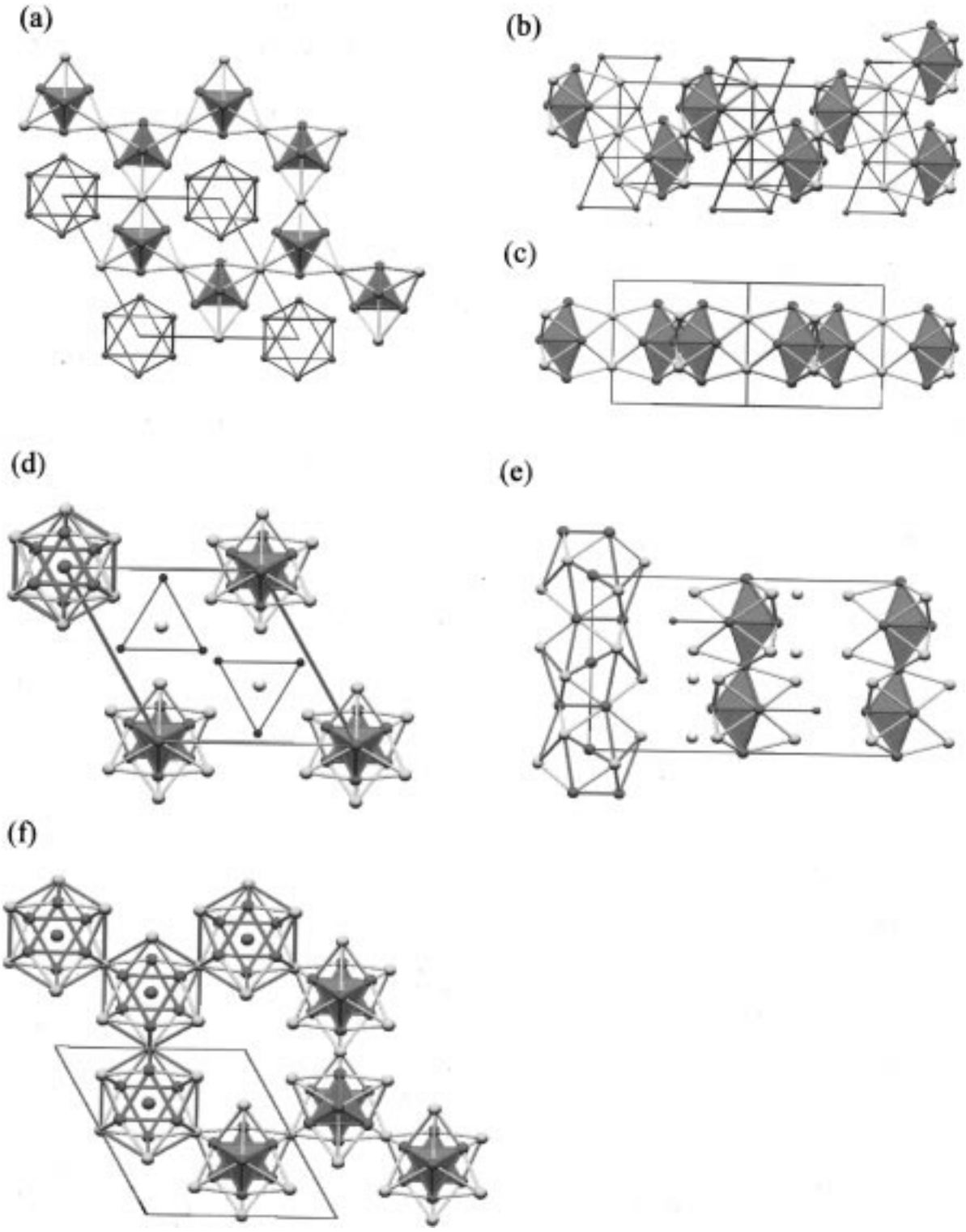

Figure 7. (a) A hexagonal framework built from DTS units sharing type C atoms as projected along [001]. In this projection two kinds of linkages can be hidden. Either each DTS cluster is linked to (b) six other clusters or (c) only to three (projections along [11$\bar{2}$0]). The octahedra represent the Ba substructure in $Ba_3Li_3Ga_{4.1}$. (d) The DTS arrangement in the structure of $BaLi_4$ as projected along [001] and [11$\bar{2}$0] (e). (f) A hypothetical framework ((001) projection) in which the DTS rods of the $BaLi_4$ structure are directly linked by common type C atoms (condensed $BaLi_4$ framework). The orientation of the rods is the same as in $BaLi_4$.

interaction is not included in the calculated stability curves. In the following we compare only amplitudes of stability curves of frameworks with the same kind of connectivity. In particular we compare the stability curve of an idealized TS/DTS framework with the one of its "stuffed" variant which includes the small fraction of interstitial atoms on high-symmetrical sites and with the one of the corresponding observed (distorted) framework.

In Figure 9a the energy difference curves for the two TS frameworks with shared type C atoms are shown. The stability curve for the open TS framework formed by the Na atoms in **NaBa** does not exhibit a maximum, indicating that there is probably no electronic reason for its formation in this compound. On the other hand, the framework with fcc arranged TS units has a distinctive maximum at 2.35 e/atom. Comparing the TS frameworks of the $\mathbf{SiF_4}$ and $\mathbf{NaZn_{13}}$ structures (Figure 9b), the

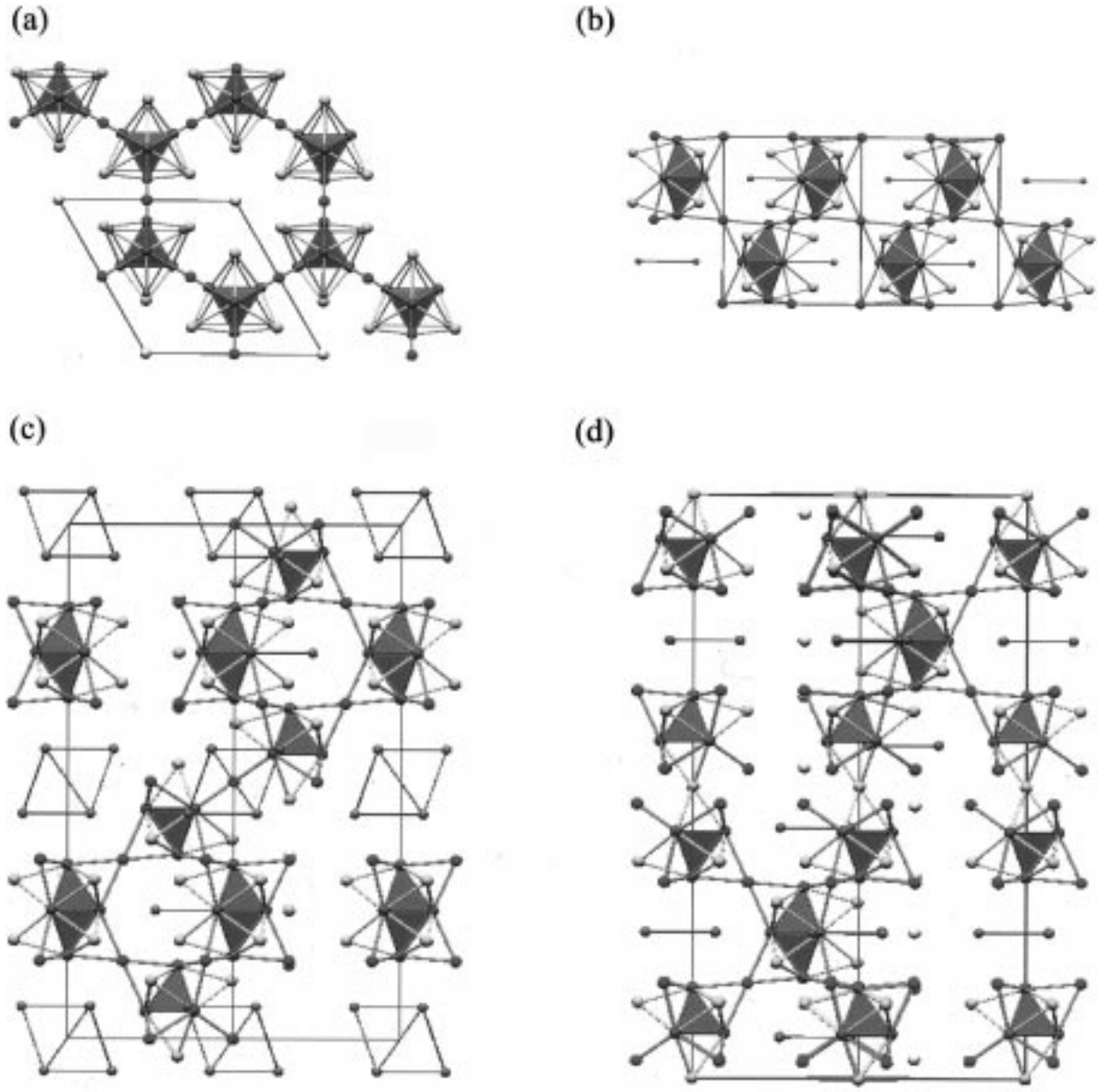

Figure 8. (a) The structures of $EuMg_{5.2}$ and $ErZn_5$ projected along [001] and along [11$\bar{2}$0] (b). (c) The structure of Sr_3Mg_{13} projected along [11$\bar{2}$0]. (d) The structure of $Sr_9Li_{17.5}Al_{25.5}$ projected along [11$\bar{2}$0]. The latter structures are related in the same way as is the pair $Th_6Mn_{23}/Ba_2Li_{4.21}Al_{4.79}$.

less dense arrangement of the $NaZn_{13}$ structures appears as the more stable solution in the range of VEC under consideration. Its maximum of stability is found at a VEC of 2.3 e/atom, that of the SiF_4 arrangement at 2.15 e/atom. The inclusion of the interstitial, icosahedra-centering atoms to the $NaZn_{13}$-TS framework diminishes the amplitude and reduces the optimum VEC to 2.2 e/atom. When assuming a charge transfer from the electropositive component, the Z frameworks in the compounds AZ_{13}, AeZ_{13}, and RZ_{13} (Z = Be, Zn, Hg) obtain a VEC between 2.08 and 2.23 e/atom which fits the calculated optimum value. The compound $BaCu_{13}$ seems to be electron deficient. The VEC of the framework in the ternary compounds also fall into this range (with the exception of $BaCu_5Al_8$ (2.38 e/atom)), and we can now explain their narrow phase widths by an optimum VEC for the framework atoms of about 2.2 e/atom. Only $LaCu_xAl_{13-x}$ is reported with a considerable phase width ($5.5 \leq x \leq 10$).[20] The range of VEC corresponding to this phase width is marked with a second bar in Figure 9b. Proceeding with the TS arrangement in **Th_6Mn_{23}** (Figure 9c) the optimum VEC of the idealized framework is 2.5 e/atom, and this value is not changed when interstital atoms are included or when the slightly distorted framework of an observed compound ($Ca_6Li_{11}Al_{12}$)[11] is considered. Again, this coincides with the VEC of the frameworks of the binary compounds Ae_6Mg_{23} and R_6Zn_{23} and the ternary compounds $Mg_6Cu_{16}Si_7$, $Ca_6Li_{11}Al_{12}$, $Pr_6Ag_{13}Al_{10}$ which lie in a range between 2.46 and 2.78 e/atom. The compounds Sr_6Li_{23} and R_6Cu_{23} are electron deficient. For the TS framework of the **$Ba_2Li_{4.21}Al_{4.79}$** structure the inclusion of the interstitial atoms has a strong stabilizing effect but does not change the position of the maximum which is found at a VEC of 2.6 e/atom (Figure 9d). The VEC of the reduced (Li,Al) framework in $Ba_2Li_{4.21}Al_{4.79}$ is 2.51 e/atom, only slightly below the optimum value. Surprisingly the icosahedron emphasizing distortion in the observed structure (c/a contraction) is of no significance to the calculated stability curve. In **$BaHg_{11}$** the distortion of the idealized TS framework in the observed structure has a stabilizing effect (Figure 9e) but affects only slightly the position of the maximum value at 2.55 e/atom. The VEC of the reduced TS frameworks in the binary compounds $AeHg_{11}$ and RCd_{11} is 2.18 and 2.27 e/atoms, respectively. The VECs of the known

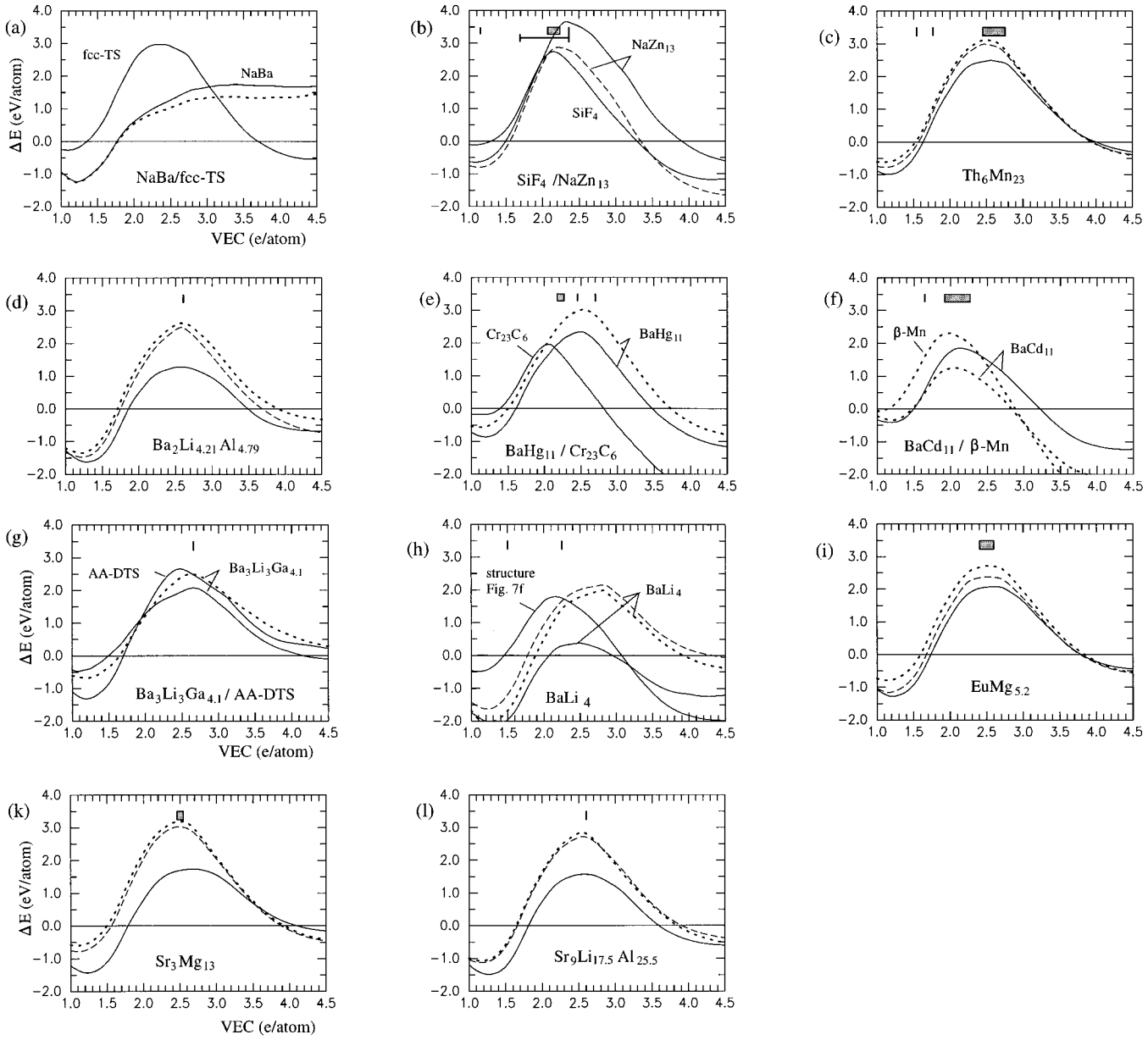

Figure 9. (a)−(l) Stability curves of the presented frameworks. Solid line curves correspond to frameworks built of idealized TS or DTS units (where possible), dashed line curves to such idealized TS/DTS frameworks where the small fraction of interstitial atoms on high symmetrical position has been included, and the dotted line curves represent the frameworks of the actual structures. The ranges of VEC as realized in sp-bonded compounds are indicated.

ternary compounds $CaAg_4Al_7$ (2.45 e/atom) and $CeAg_{3.1}Al_{7.9}$ (2.70 e/atom) are much closer to the calculated optimum value. The TS framework of the **$Cr_{23}C_6$** structure has its stability maximum at the very low VEC of 2.05 e/atom (Figure 9e). This fact together with the lack of large voids turn this framework into an unlikely candidate for a sp-bonded system, and indeed no representative is known. The framework of the **$BaCd_{11}$** structure built from TS strands has its stability maximum at a VEC of 2.1 e/atom (Figure 9f). The interstitial atoms have a destabilizing effect but do not change the position of the maximum value. When estimating the VEC of the reduced frameworks of the binary compounds AeZ_{11} and RZ_{11} (Z = Cd, Zn), we obtain values of 2.18 and 2.27 e/atom, respectively. For the frameworks of the known ternaries VEC is between 1.91 and 2.18 e/atom, with the exception of $NdCu_9Al_2$ (1.64 e/atom). The *β*-**Mn** structure as "collapsed" $BaCd_{11}$-TS framework has the maximum at a slightly lower value. The optimum VEC for a sp-bonded system with this structure would be 2.0 (Figure 9f). For a DTS framework as it might occur in **$Ba_3Li_3Ga_{4.1}$** this optimum value is found to be 2.65 e/atom for the idealized case (Figure 9g). The calculation of the stability curve with the atomic positions of $Ba_3Li_3Ga_{4.1}$ yields the same value which coincides precisely with VEC following from the composition of $Ba_3Li_3Ga_{4.1}$ (2.66 e/atom). This finding supports the structural model based on a DTS framework but does not give an explanation for the unsymmetrical occupation of the T^{ax} atom position in this compound.[40] The alternative linkage, leading to a graphite-like layer of DTS units, has in the case of an AA stacking sequence an optimum value of VEC at 2.45 e/atom (Figure 9g, in this figure the alternative linkage to $Ba_3Li_3Ga_{4.1}$ is abbreviated with AA-DTS). Of all investigated examples of TS and DTS frameworks the stability curve of the idealized framework of the **$BaLi_4$** structure is most influenced by interstitial atoms (Figure 9h). Its amplitude is greatly

(50) Hofmann, P.; Nesper, R. *COLTURE: program for interactive visualisation of crystal structures*; ETH Zürich: Zürich, Switzerland, 1995.

increased and the position of its maximum value shifted from VEC = 2.5 e/atom to 2.8 e/atom. The representatives $BaLi_4$ and $CaZn_3$ with a framework VEC of 1.5 and 2.24 e/atom, respectively, appear both as electron deficient compounds. The optimum VEC of the more dense framework in a hypothetical structure where the DTS rods are directly linked together (Figure 7f) is about 2.15 e/atom. For the DTS framework of **$EuMg_{5.2}$** and **$ErZn_5$** the optimum VEC is found to be 2.5 e/atom (Figure 9i). The inclusion of the interstitial atoms leading to the composition 1:5 (cf. section 5.2.3) does not affect this value. On the basis of this idealized composition the VEC of the frameworks of the reported compounds $EuMg_{5.2}$, $Eu_{0.33}Sr_{0.67}Mg_{5.2}$, $SrMg_{5.2}$, and RZn_5 (R = Lu, Ho, Er, Tm, Eu, Y) are in a range between 2.4 and 2.6 e/atom which fits the calulated optimum value. The mixed TS/DTS frameworks of the **Sr_3Mg_{13}** structure has its maximum of stability at 2.65 e/atoms (Figure 9k). When considering the interstitial atoms this framework is stabilized and the optimum VEC reduced to 2.5 e/atoms. The VEC of the frameworks of the two representatives Sr_3Mg_{13} and $EuSr_2Mg_{13}$ are 2.43 and 2.53 e/atom, respectively. Finally in Figure 9l the stability curve for the TS/DTS framework of the **$Sr_9Li_{17.5}Al_{25.5}$** structure is shown. The maximum value at VEC = 2.55 e/atom is not influenced by the interstitial atoms. The actual VEC of the framework in $Sr_9Li_{17.5}Al_{25.5}$ is 2.60 e/atom.

Summarizing the results of these calculations it appears indeed that the relative stability of the investigated TS/DTS frameworks is strongly dependent on VEC (with the exception of the NaBa framework). The frameworks exhibit a pronounced maximum of stability in the range of 2.1−2.6 e/atom with the particular optimum values slightly depending on the kind of basis cluster and its connectivity. Remarkably, these optimum values follow in most cases already from the idealized model structures, and distortions of TS/DTS units in observed structures are of minor influence. When applying a formal electron transfer from the more electropositive component to the framework in the corresponding intermetallic compounds, we obtain values of VEC which are very close to the calculated optimum ones. Ternary compounds where the divalent metal of the majority component is replaced by a combination of a mono-(I) and trivalent(III) metal have the possibility of "fine-tuning" the framework VEC toward the optimum values via the flexible I/III ratio. The clear tendency of this class of compounds to achieve an optimum VEC for its substructures is in the spirit of the Zintl−Klemm concept. However, it must be emphasized that VEC is an even weaker factor for determining structural stability than it is for the more electron rich polar intermetallics with substructures solely formed by the more electronegative Tr atoms.

7. Concluding Remarks

We could show that the presented family of sp-bonded intermetallic compounds consisting of a framework formed by electronegative divalent metals or combinations of a mono- and a trivalent metal and large-sized counteratoms still resemble Zintl phases and thus can be counted as electron compounds. As in the more electron rich polar intermetallics with substructures based on deltahedral clusters, the frameworks in these compounds also appear in a reduced form and the resulting electron count adjoins that of the more electron rich intermetallics. Completely different however is the origin of the structural diversity of these two classes of sp-bonded intermetallics. Whereas structural diversity of the more electron rich polar intermetallics originates in the formation of a large variety of different cluster units, the one of the presented, electronically adjoining, compounds is based on the linkage possibilities of only two basis clusters. The basis clusters TS and DTS appear as flexible building units and account for numerous possible frameworks, including different icosahedral aggregates. The kind and connectivity of the basis clusters determine the number and size of voids in the framework hosting the electropositive counteratoms and thus are responsible for the stoichiometry of the intermetallic compound. The exploration of systems with two different electropositive components is expected to give valuable information about the influence of size and packing effects in these TS/DTS based systems.

Acknowledgment. This research was supported by the Swedish National Science Research Council (NFR). U.H. acknowledges a Feodor-Lynen Fellowship of the A. v. Humboldt Foundation.

Supporting Information Available: Crystallographic data (1 page, print/PDF). See any current masthead page for ordering information and Web access instructions.

JA973335Y